Delft University of Technology

Bachelor Thesis
AESB3400

Core Analysis and Well Data Interpretation for Facies Extrapolation with a focus on coals and coarse sand in the Carboniferous of the Southern North Sea

Author:
Rutger Treur (4555422)

April 11, 2020

I promise that I have not used unauthorized help from people or other sources for completing my exam. I created the submitted answers all by myself during the time frame that was allocated for the Bachelor End Project AESB3400.

Contents

1 Abstract **3**

2 Introduction **4**
2.1 Geological Background . . . 5
2.2 Well Log Analysis and Extrapolation Techniques . . . 7
2.2.1 Gamma Ray Logs . . . 7
2.2.2 Sonic Logs . . . 7
2.2.3 Correlation Techniques . . . 8

3 Methods **9**
3.1 Workflow . . . 9
3.2 Data Gathering . . . 9
3.3 Well information . . . 9
3.4 Data Formatting . . . 10
3.5 Data Analysis . . . 11
3.6 Facies Extrapolation . . . 11

4 Results **13**
4.1 Core Logging . . . 13
4.1.1 Core Logs . . . 13
4.1.2 Core interpretation . . . 13
4.2 Well logs and core comparison . . . 17
4.3 Data analysis and PCA . . . 17
4.3.1 Swamp facies Results . . . 17
4.3.2 Channel Base Facies Results . . . 22
4.4 Extrapolation in the Well . . . 23
4.4.1 Swamp Facies Extrapolation . . . 24
4.4.2 Channel Base Facies Extrapolation . . . 24

5 Discussion **26**
5.1 Core Logging & Interpretation . . . 26
5.2 Well logs . . . 27
5.3 Core/Well Logs Correlation . . . 27
5.4 Data analysis and PCA . . . 27
5.5 Well Facies Extrapolation . . . 28

A Well logging Suite over a longer interval **32**

B Interpretations from drilling geologist **33**

C MatLab script for initial analysis of cored interval **35**

D MatLab script for well extension **39**

1 Abstract

In 1990, the 44/21a-6 well was drilled in the Southern North Sea. Core material was taken from the Westphalian A/B part of the core. Some of this core material was recently obtained by the TU Delft via the North Sea Core Initiative. Since the Westphalian A/B in the Pennine Basin is fluvio-deltaic in origin, it is highly variable both vertically and laterally. In this thesis we set out to develop a method to extrapolate facies found in the core material to recognize if these are present in other locations in the well. This means that core material is correlated to the well log. This correlation is then extended over the rest of the well. Two investigation targets were chosen, the first facies is channel base facies, consisting of very coarse sandstone, the second a swamp facies. This firstly requires a detailed core log, and a short study of the well log data. The core log is interpreted in order to try to establish some form of elektrofacies. The well data is then formatted and different principal component analyses (PCA's) are performed in order to differentiate the facies from their surroundings. For both analyses more than 90% of the variance was explained by the first two component axes, making them reliable. Both target facies require different data sets in order to distinguish them from their surroundings. The swamp facies becomes easily visible from the third principal component axis, while the channel base sand is harder to differentiate, being recognizable from a point cloud in a principal component plot. In total 40 coals were found to be present over the researched well interval, starting underneath the Zechstein formation, from 12800 to 13800 ft. No other similar channel base coarse sands were found over the interval apart from the one in the cored material. Overall, it seems that the basics for this method of detection and extrapolation is quite reliable and better than using the original log data, although it does need some further development and improvement.

2 Introduction

Climate change is for this world is nothing new. It is widely known these days that the earth's climate has varied over most of its history. This is an interesting fact if we want to be able predict some of the effects of the climate change we see today. We can study the climate of the past by looking at the earth's geology. Many clues to the effects of climate change are preserved in the earth we walk on every day. In this study, we will be focusing on the Carboniferous in the southern North Sea. In order to extract information from the earth, from the Carboniferous in this case, we first have to know what is present underground. This is an issue that is widely spread throughout geology, since we collect data that is spatially sparse, but try to extract 3D geological information from it.

This problem is nothing new, it has existed since the dawn of geology. However, new tools have introduced new ways of gathering data from the earth in the second half of the twentieth century. Many of these tools primary uses were focused hydrocarbon exploration and they provide a rich source of data for geologists. Instead of physically looking at rocks, geophysical measurements provide clues to the nature of the subsurface.

In the southern North Sea, these tools have also been widely in hydrocarbon exploration. A good overview of these efforts, although not the most recent, is given by Cameron et al. (2005). In most of the wells drilled well logging was performed. Using these well logs, facies can be constructed from digital data instead of outcrops. However, although many methods exist, not all of them are reliable. Using Gamma Ray (GR) logs as a facies indicator for example, has been criticized by Rider (1990).

Using the data from these explorations to extract information from in the southern North Sea appears to be commonplace. O'Mara (1995), O'Mara & Turner (1997), Collinson et al. (1993) and Hampson et al. (1999) to name just a few have used the well logging data in their geological research on the Carboniferous. All of these have used the data to identify layers and facies to correlate between wells. However, no research could be found on the smaller scale, on how the Carboniferous rock specifically responds on well logs.

Also, no research could be found that applied principal component analysis to well logging responses, although some work has apparently been done using this analysis method on other sandstones in different applications, although it seems uncommon. Most of this work focused on the mechanical and reservoir properties of sandstone, such as the paper from Huang et al. (2018). Most of these papers are quite recent as well.

That raises the questions which are central in this thesis. 'How can we link the facies from well core and well logs in the 44/21a-6 well?', 'How can we reliably extrapolate using this link?' and 'How accurate is our method?'. We hypothesize that it should be possible to link these facies using principal component analysis, and that we can extrapolate by using a script using that same principal component analysis. We also think that it should be possible to accurately predict at least half of the coals in the well and half of the coarse sand.

Thus, this bachelor's thesis is on the Carboniferous in the southern North Sea. This is done as part of a broader project into the matter currently running at the TU Delft. This project is done to make interpreting the data from the Westphalian A/B interval easier, as a lot of variability is present, both vertically and laterally. A lot of the work done builds on the master's thesis by O'Mara (1995). This introduction will give the necessary background information to the topic. Firstly, we will give some background information about the studied well interval. Secondly, we will be discussing the geological setting in which the interval was formed and deposited. Thirdly, an introduction to the well correlation techniques used is given.

2.1 Geological Background

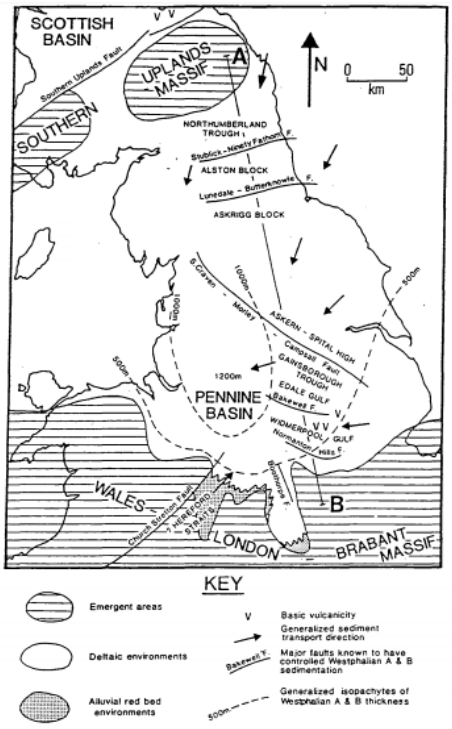

Figure 1: Generalised palaeogeographic map of the Pennine Basin during Westphalian A and B times. (by O'Mara (1995) after Guion & Fielding (1988))

The Carboniferous of the southern North Sea has been quite extensively studied over the years, mainly with a focus on the exploration potential of the gas that is found in many places, such as by Cameron et al. (2005), although other studies have also focused on more geological features such as the studies from O'Mara & Turner (1997). The Carboniferous of the southern North Sea has long been known as a gas producing region, and as such quite a lot of data is available publicly from this region. We also find outcrops of the Carboniferous in England as well as in many parts of Europe. (Leeder & Hardman, 1990), and these outcrops are very similar to what is found in the North Sea wells. Collinson et al. (1993) has also very well outlined the different phases in the Carboniferous, and according to that study the cored well interval can be placed along the lower boundary of the Westphalian A/B. The cored sediments are of fluvial origin. To give an idea of the environment in which many of these sediments were deposited, a general outline of two relevant river systems is displayed in figure 2. These are meandering (2b) and braided rivers(2a).
The rocks in this interval are thus known to have formed in the Pennine Basin. This basin was formed from a foreland basin in the Variscan orogeny, which spread north. It was then in some places infilled with limestones. In the Namurian, subsidence patterns became more uniform into the Westphalian, although some syn-depositional faulting was still present. This stopped just before the formation of Pangaea was complete. (O'Mara, 1995)
In summary, the basin is part of a large retro-arc structure. The basin was immediately to the north of the older rigid Anglo-Brabant High and is south of the extension to the Southern

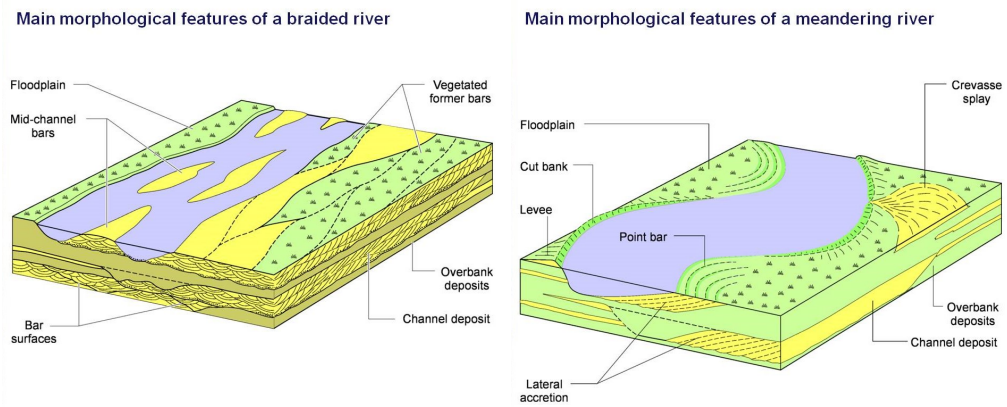

(a) Schematic of a braided river.

(b) Schematic of a meandering river

Figure 2: figure showing two river systems, indicating the different features. Figures from Nichols (2009)

Uplands, with its granite core. It can be best seen as an eastern continuation of the Pennine Carboniferous Basin which lies south of the tilt blocks of the nothern Pennines and north of the stable Welsh-Anglian-Brabant High. There are two subbasins which are separated by the East Midlands 'Shelf', which in turn is an area of relatively slow subsidence, intruded by the Newark and Market Weighton granitoids. (Leeder & Hardman, 1990). This is illustrated in figure 1.
The lowest parts of the Carboniferous, the Dinantian, varies from thick fluviatile redbed sequences of Old Red Sandstone to alternating clastic/limestone sequences of fluvio-deltaic/marine cycles of Yoredale aspects. (Leeder & Hardman, 1990).
The Namurian shows regional change from these Yoredale facies in the North to a typical Millstone Grit facies in the south, although the transition is still to be well-documented offshore. Turbidites are important elements in the infill of the early Namurian. In the area, much of the Namurian shows upward coarsening sequences similar to those associated with 'sheet delta' progradations onshore. (Collinson et al., 1993)
The Westphalian can be subdivided into the Westphalian A/B and the Westphalian C/D. A generalized map of the paleogeography in the Westphalian A/B is shown in figure 1. In the southern portion of Quadrant 43 the Westphalian A/B can be as thick as 1000 m., although it thins southwards onto the flanks of the Anglo-Brabant High. These sediments are mostly fluvio-deltaic in origin, although marine mudrocks are common in the Westphalian A. Fluviatile sandstones show an increase in grain size eastwards through the entire Westphalian A/B. In the Westphalian B stacked channel sandstones are common in the southern part of Quadrant 44.(Leeder & Hardman, 1990) Coal bearing layers can be quite common in this part of the Westphalian as well. (Collinson et al., 1993)
Sandstone and channel sandstone abundance and channel dimensions patterns suggests that sediment was delivered to the basin from more than one direction. These influences are especially clear for the Westphalian A/B as a result of the better data quality there. The dominant source lay to the north and supplied by far the greatest volumes to the basin throughout the whole Carboniferous. A second source lay southeast and the third source was the Anglo-Brabant Massif which spread smaller amount of sediment to a relatively narrow strip along its northern margin. This suggests that the southern North Sea was a major depocentre to which several sources supplied sediment, with a diminishing number of channels penetrating all the way to

the centre of the basin. (Collinson et al., 1993) The Westphalian A/B is further characterized by the disruption of the sequence by 19 marine bands which are found all over europe and on land are used for identification. These bands were formed by sudden sea level changes, which are hypothesized to be third and fourth order changes. On land, these marine bands are often used for identification. (O'Mara & Turner, 1997)
In the Westphalian C/D most of the sandstones are of fluvial origin, very few coals and marine shales are present compared to the Westphalian A/B. The Westphalian C/D is dominated by mature sandstones and red floodplain mudrocks with dessication cracks. This part of the Westphalian is also often referred to as the 'Barren Red Measures'. (Leeder & Hardman, 1990)

2.2 Well Log Analysis and Extrapolation Techniques

As drilling techniques improved in the twentieth century, well logging became customary as a way to improve the amount of data gathered from each well. In this project, well logging data is used to recognize different lithologies and extrapolate this to different wells and different intervals. This is done using many of the instruments available. In this report, the detection of coals relies heavily upon the use of two instrument, which we will therefore cover into detail here. These are the sonic logs and the gamma ray application. For the recognition of sands, a much broader suit of measurements is needed and therefore these instruments are not covered separately. O'Mara (1995) gives recognition patterns for different sandstone facies on well logs, but these patterns were not observed on our cored interval. Therefore, for the recognition of sands, we do not directly rely on the well logs.

2.2.1 Gamma Ray Logs

The gamma ray tool measures the natural radioactivity. The rocks in the earth contain many elements, many of which have more than one isotope. As a result, many of these elements are not stable and emit alfa, beta or gamma radiation. This radiation is emitted and can even pass though well casings. This radiation is then picked up by the receiver in the gamma ray instrument and converted to an electrical signal. Because the natural radioactivity varies randomly over time, averaging is applied by digital means. Because the elements emit radiation at different energy levels, these logs can be split into different signals, giving the uranium, thorium and potassium fractions in the surrounding rocks. If they are not split out into different energy levels, the total radioactivity is generally measured in API. These units are defined from a pit at the university of Houston Texas. The API Gamma Ray unit is 1/200 of the difference in log deflection between the two zones of different gamma ray intensity in the pit, where there are zones of high and one low radioactivity. These instruments are used to detect layers with high radioactivity, which can be layers with high organic contents such as coals, or layers with large amount of shales, which are generally also highly radioactive.(Wolf, 1999) If we look at the studied well, which consists of many types of shales, sandstones and coals. From these lithologies, sands give a good baseline for the Gamma Ray log. Although sands can be contaminated with radioactive minerals, this is rare and therefore most sands give a stable, low GR reading. This is different for coal, which is often rich in uranium, and for shales, which are often rich in thorium and potassium. Although exceptions to these rules do occasionaly occur, there is no reason to think this would be the case for the rocks studied in this report.

2.2.2 Sonic Logs

The sonic logs measures the speed with which waves can propagate through a medium. It does however not measure this in velocity, but rather in its inverse, travel time, in μsec/ft. This means

that in media which have very fast speeds, the tool will output low scores, while slow media will score high. Basically, this speed is measured between a transmitter and a receiver, but tools with more sets of receivers and transmitters to get more accurate data are commonplace. A transmitter generates compressional (P) waves and shear (S) waves. These waves are emitted into the borehole wall where they travel at a certain speed through the formation before being reflected back into the receiver. Only the P waves are measured at the receiver, since to get to the transmitter the waves must travel through the borehole fluids which do not sustain shear. The travel times are then logged and corrected for the spacing between the transmitter and receiver. These corrected times are then logged as data. Travel times generally vary based on the composition of the rocks they travel. Very high density and low porosity rocks give low travel time as the wave can easily propagate, whereas very low density, organic materials possibly with a high porosity give very high travel times. This means that coal in particular will get a very high reading, as it has a low density causing long travel times. For shales and sands, whose densities are often very similar, travel times do not often show differences. (Wolf, 1999).

2.2.3 Correlation Techniques

From all the data described above, as well as the cores that might be available from certain wells we can construct a lithology. Doing this for more than one well can give quite a few data points. The next step would be to connect the dots, working from the assumption that all layers are laterally continuous and should thus be visible in multiple wells. So, by comparing log responses it is possible to construct a 3D subsurface topography in its simplest form. However local variability, for example from meandering rivers or faulting can complicate this environment very strongly as many layers are not continuous. Therefore, we have to look for similar features in both well data sets signifying similar lithologies or facies. There are many ways to do this, from simple guesstimation to complicated statistical approaches.

3 Methods

In this section we will be discussing the workflow and methods used in this thesis. Firstly, we will be discussing the workflow as a whole to give an overview of the activities undertaken in this thesis. Secondly, we will be discussing the data gathering activities from the workflow in more detail where necessary. Thirdly, we will be discussing the data formatting and processing. Fourthly, we will look into the process of analyzing the results and doing some well correlations based of these.

3.1 Workflow

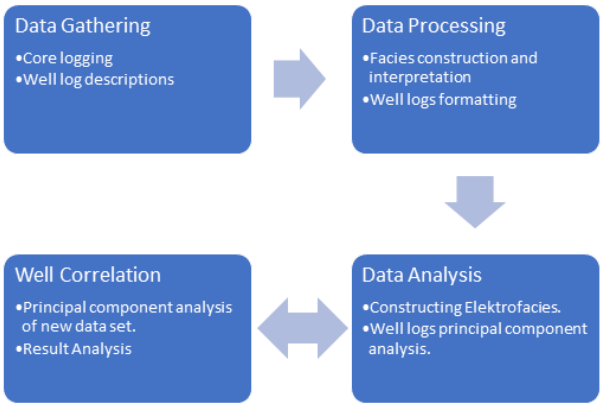

Figure 3: Workflow for the project.

The workflow for this project is shown in figure 3. As can be seen this project involves three basic steps involved in every project. These steps are further explained in the following sections. As is to be expected, the lines between the different phases of the project are not always as clear as they might seem. For example, well correlation and data analysis are innately related because in data analysis we will be looking for features which can be used in well correlation. As such the well correlation feeds back into the data analysis.

3.2 Data Gathering

The data gathering step for this project is twofold, as there are two data sets used in the project. Firstly, there is the core logging. This is done on a piece of core from the well 44-21a-6. The cored interval which is available is the section from 13205-13315 ft. This section is studied carefully, in order to construct a well log. This well log is on cm-scale, giving a detailed description of the core.
Apart from this, we are making use of the logging data which have been gathered from the well. This data is publicly available. The data for this well has been logged at half foot intervals, giving a reasonable enough resolution.

3.3 Well information

The studied well interval is from the UK, from the 44-21a-6 well. This exploration well was drilled in 1990 in the southern North Sea. It is located at 54.218575°N, 2.18225°E. The well

location and the quadrants are displayed in figure 4. The well data are publicly available from https://ndr.ogauthority.co.uk/. (Oil and Gas Authority, 1996) The studied well core is from the depth interval of 13205 to 13315 ft. The core slab was donated to the TU Delft by North Sea Core Initiative, Aberdeen, UK, see also https://northseacore.co.uk

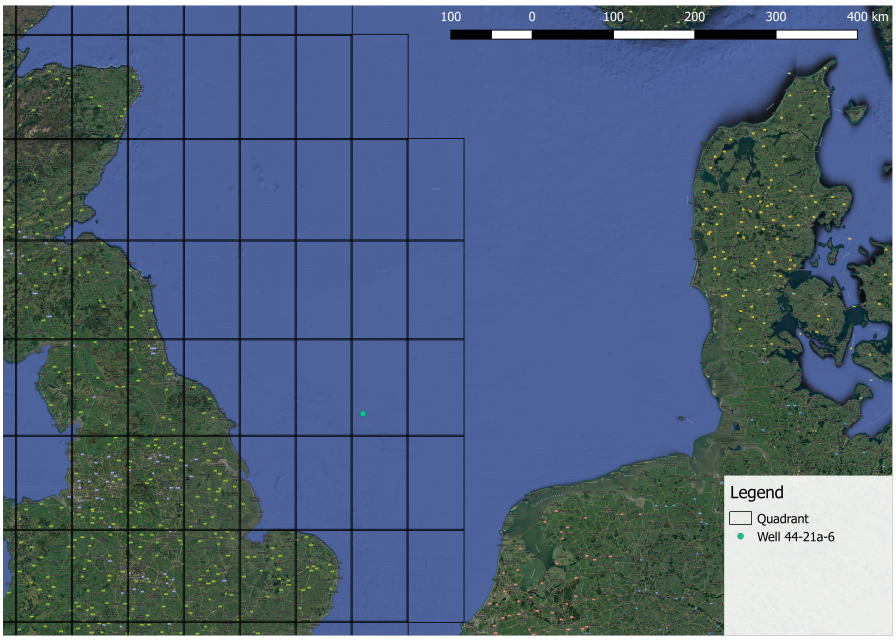

Figure 4: Well location map.

3.4 Data Formatting

Data processing of the data mentioned above is a more elaborate process. From the core litholog we need to group our measurements into intervals, based on lithology. From these groups we construct facies, which can tell us something about the depositional environments of these intervals.
Here we also need to format our well log data in order to be able to use it in the analysis. This means that useless data will be removed. This means that the GR and induction logs (only for the coal analysis), as well as the tension logs are removed from the data as they corrupt the analysis. Why these logs are removed is further discussed in section 5.4. Also, the well logs are edited to remove locations where not all measurements are included. This means that in the analysis the following measurements must be included in the order displayed in table 2 for the analysis of the coaly layers, and the form of 1 for the analysis of the sands.

Log Type	1. Caliper	2. Sonic	3. Gamma Ray	4. Induction	5. Neutron Porosity	6. Potassium	7. Density	8. Thorium	9. Uranium
Log Header Name	CALI	DT	GR	ILD	NPHI	POTA	RHOB	THOR	URAN
Log Unit	inch	μsec/ft	API	ohm-m	%	PPM	gr/cm3	PPM	[-]

Table 1: Table of necessary data format for coarse sand analysis.

Log Type	1. Caliper	2. Sonic	3. Neutron Porosity	4. Potassium	5. Density	6. Thorium	7. Uranium
Log Header Name	CALI	DT	NPHI	POTA	RHOB	THOR	URAN
Log Unit	inch	μsec/ft	%	PPM	gr/cm3	PPM	[-]

Table 2: Table of necessary data format for coal analysis.

Since many well logging companies have their own formats for the data that is delivered, it is probable that at least some amount of data pre-processing is required in order to make the analysis as done here possible. This can be done effectively using excel or other tools. Since we are trying to link the core logs to the geophysical well logs, the last step in this process is to identify the cored interval in our well test data. This cored interval is known to be from 13205-13315 ft. Since we can identify the small coaly section seen in the core easily on the logs, as explained in sections 4.1 and 4.2, we can also calibrate the depths in the well logs, although it could also be done the other way around, by changing the depths on the core. We know that the real depth of the coal interval is about 13264 ft. from the core photos, but it does not show up in the logs until 13275 ft., so we choose to move the well logs up by 11 ft. in order to make them correspond. This is a rather important step in being able to link the logs and the core.

3.5 Data Analysis

When all the data is in the right format and the depths are corrected, as described in the previous section and illustrated in table 1 or 2 depending on the target, it can be used for analysis. The analysis method of choice here is principal component analysis (PCA). We apply this method to the cored interval first, because from there we can validate the results using the core logs. Using this method we decrease the dimensionality of the data from a 7-D to a 3-D data set for the coaly interval, and from a 9-D to a 2-D dataset for the sands. This can be done because PCA groups the vast majority of variance into the first two or three data dimensions. This is important to make the data set more readable and easier to use. This makes analysis much easier because of the reduced dimensionality. However, some parts of the analysis get harder because it is not easy to predict what variability ends up where in the end. That is why it needs to be compared to the well core to make sure the right features are highlighted.
Doing this analysis requires computer programming, and in this we choose to use MatLab, as it has a built in PCA function. The script to do this is included in appendix C. The analysis will output a score matrix, a transformation of the original data but now aligned along the principal component axes. This means that we get a new 7-D or 9-D data set. However, as it turns out only the first couple of components actually contain useful data in these cases, as expected. The second output is the coefficients matrix, which indicates how the principal components are related to the original logs by giving the coefficients for the linear combinations which form the principal components. The third output is an array which gives the variances explained by each principal component. This data can be used to analyse the usefulness of the PCA results.
The score matrix can now be plotted against depth to identify what features from the core can be identified from what principal component. Also, the first and second principal component can be plotted against each other, which gives clouds of data points which can identify certain features, such as lithology.

3.6 Facies Extrapolation

In order to extend certain features from the core to the rest of the well, we will apply the same principal component analysis to the rest of the well. This means that the logs first have to be

centered. In this case that means that we are substracting the mean of the cored interval from each column. That is because we want our principal component analysis to be comparable to the cored interval and therefore we use the same principal component constructions. Having subtracted this mean, we multiply the $7 * depth$ data set with the $7 * 7$ coefficient matrix in order to get our principal component scores for the complete well, in the case of the coal analysis. If we want to asses the sands we multiply the $9 * depth$ data set with the $9 * 9$ coefficient matrix. As mentioned before, our coals are identifiable from the third principal component. By looking at the peaks in this component, we can identify the coals that are present in the well. This is done automatically using the 'findpeaks' MatLab function, which is from the signal processing toolbox. By specifying the peak prominence, small peaks from the noise can be filtered out to quite some extent. For the sands we can plot the first and second principal components against each other, where the lithologies will separate into point clouds. Then we can mathematically define a lithology as points fitting inside an ellipse, and in that way classify them. In order to refine this process we can use this information in the data analysis steps. In this way we can iterate the process in order to, for example, optimise the peak prominence in the 'findpeaks' function.

4 Results

In this section we will be discussing the results obtained, we will firstly go into the results from the core logging. Second will be the results from the well log analysis. Thirdly, we look at the processed data and how it can be used in correlation.

4.1 Core Logging

A C=core litholog was completed on cm-scale, noting the many small scale structures present in the cores. This was done over the whole core, but it should be noted that some sections of core were missing, ranging from entire three ft. slab sections to small samples (10 cm height, 5 cm diameter).

4.1.1 Core Logs

The results of the core logging are in figure 5, where the intervals on which logging took place are specified, as well as observed structures and other notes. As can be seen from the figure, the core has several distinct layers. It includes five sand layers, four shales and one coaly layer. Between these sands there are roughly three catergories of sand. Firstly, there is the upper medium sandstone, which has lots of low angle and flat lamination. This is found from the top at 13205 ft. all the way to 13223 ft. Secondly, below that we find a remarkably coarse interval, with an average grain size of a very coarse sandstone. This sandstone is about 14 ft. thick, stretching from 13223 to 13237. Thirdly, there is about 51 ft. of finer sandstone, divided over three intervals, 6 ft. from 12244 to 14250 ft., 13 ft. from 13251 to 12264 ft. depth and 32 ft. from 12266 to 12298 ft. depth, often including wavy or angled lamination. Plenty of other structures can be observed in this sand as well, like burrows and mud drapes.
We also find 4 shales in this core, 6 ft. from 12236 to 12242 ft., 1 ft. from 13250 to 13251 ft., 2 ft. 13264 to 13266 ft. and 17 from 12298 to 13315 ft. in depth, in total about 26 feet. These shales are all similar, apart from the last piece. The first 3 pieces are all silty mudstones, with a range of structures visible in them, from structureless to wavy laminated, sometimes including organic matter lamination or burrows. The last shale is different, consisting of horizontally laminated mudstone.
Lastly, we find a thin (1/2 ft.) coaly mudstone interval at 12264 depth. This piece is different from the shale which it overlays in colour, having the remarkable black coaly colour. This piece has a flat layered or laminated structure in it. The origin of the material could not be determined from this small interval.

4.1.2 Core interpretation

Since we already know that most of these layers were formed in a fluvial environment, we can interpret our core in that context. In the core we can interpret 5 separate facies. They are discussed below.

Channel base facies This facies we find at only one place in the interval from 13224 to 13237. It has in this case a thickness of 13 ft. (4 m.) which is a pretty typical thickness for this kind of deposit. (Collinson et al., 1993). This facies is characterized by its very coarse mean grain size, interspersed with even coarser grains in some places. It is generally structureless, probably due to the coarse grain size, as structures in coarse grained environments are not easily formed and preserved. (van den Berg, 2010) Some very small scale (1 cm.) flat laminated structures can sometimes be observed, but they are quite short and do not stretch the width of the core.

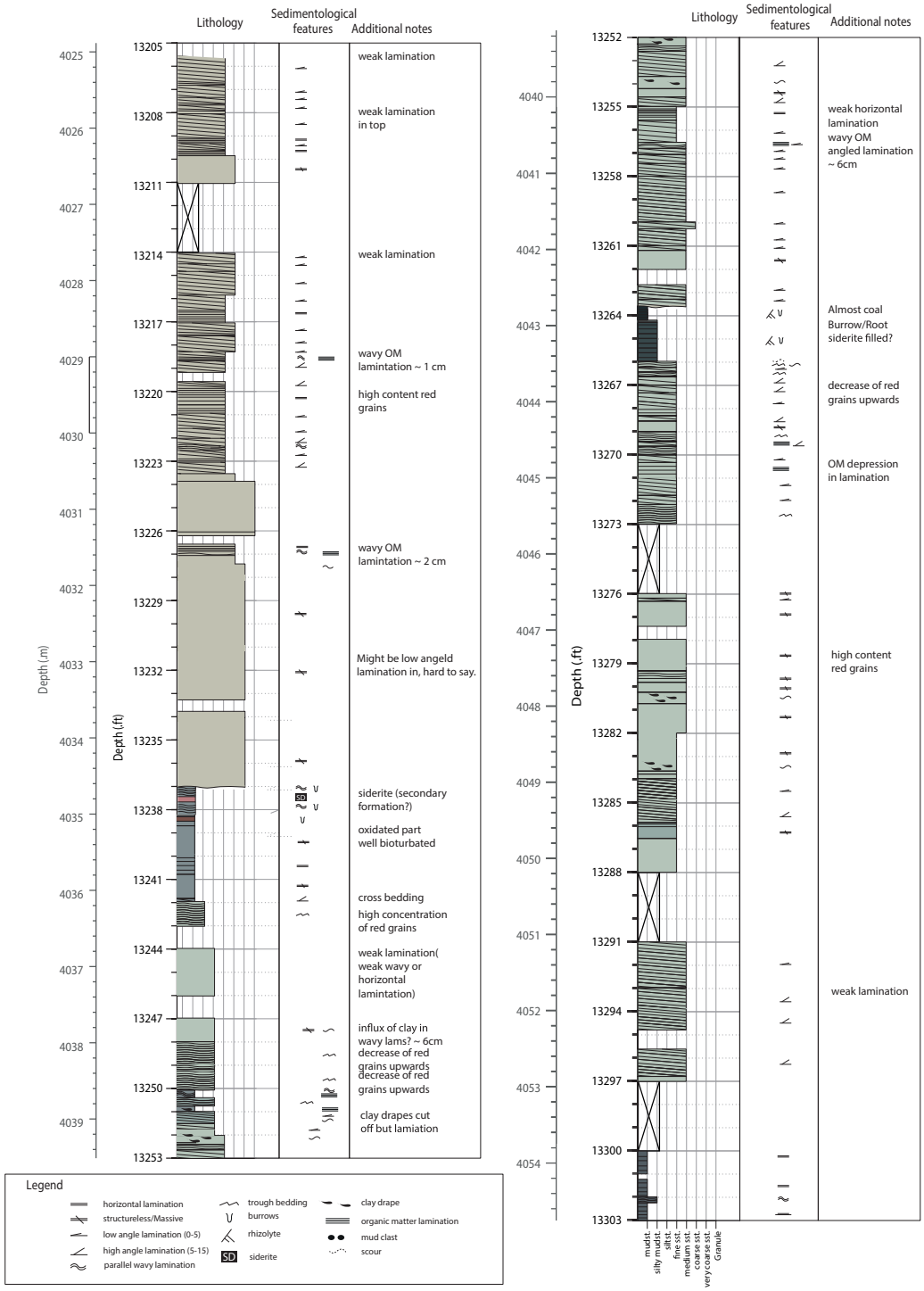

Figure 5: Core Log over the entire interval, note the missing pieces.

(a) Example of the channel base facies.

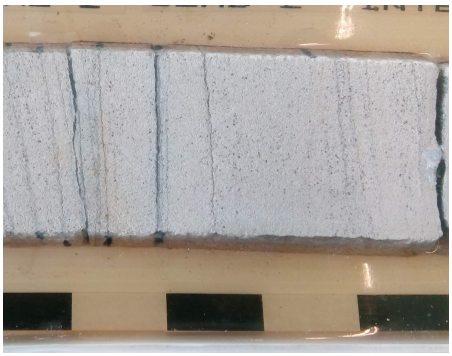

(b) Example of the channel bar facies.

Figure 6: Examples of the two sandstone facies present. The bars are 1/10 ft. long.

This facies has an erosional base with scour marks present. It can overlie any other facies, as the channel cuts into the layers below. It is generally overlain by the channel bar facies described below, as the river moves and with it the channel base. A photo of an example of this facies is included in figure 6a.

Channel bar facies This facies is found in four separate locations in the core, they are fine to medium sandstones with lots of wavy, angled and flat lamination. It is present from 13205-13223 ft., 12244-14250 ft., 13251-12264 ft. and 12266-12298 ft. depth. The facies is characterized mainly by the many structures which indicate sub-aqueous bedforms. The grain sizes differ somewhat between the intervals (fine to medium sand), but not by too much. Other structures apart from laminations are also very common in these intervals, such as mud clasts and mud drapes as well as burrows and rhyzolites. This facies is the most common in the cored interval. It is always overlain (in the cored interval) by a floodplain facies. It can overlie any of the other facies described here, although scoured or erosional bases are common. A photo of an example of this facies is included in figure 6b.

Floodplain facies We find several examples of this facies in the cored interval. It is present from 12236-12242 ft., 13250-13251 ft. and 13264-13266 ft. This facies is characterized by its grainsize, consisting of silty mudstone. It also contains quite a range of structures, including wavy, angled and horizontal lamination. Some structureless intervals are present as well. In this case they are quite thin, with the thickest being 6 ft. This facies in thought to be a floodplain deposit because of its low thickness, thin layers and the structures which indicate some flow to be present at the time of formation. In this core it overlies the channel bar facies every time. It normally underlies one of the two sandstone facies, but this boundary is often erosional. A photo of an example of this facies is included in figure 7a.

Lacustrine facies This facies is found in the core from 13000 to 13315 ft., it consists of mudstone which is horizontally laminated and is generally somewhat darker in colour than the floodplain facies. In the core 15 ft. of this facies is present in one interval, but from the well logs it looks like it is much thicker than this, at around 30 ft. This facies is thought to be of lacustrine origin because of its much greater thickness than the floodplain deposits and its structure, which,

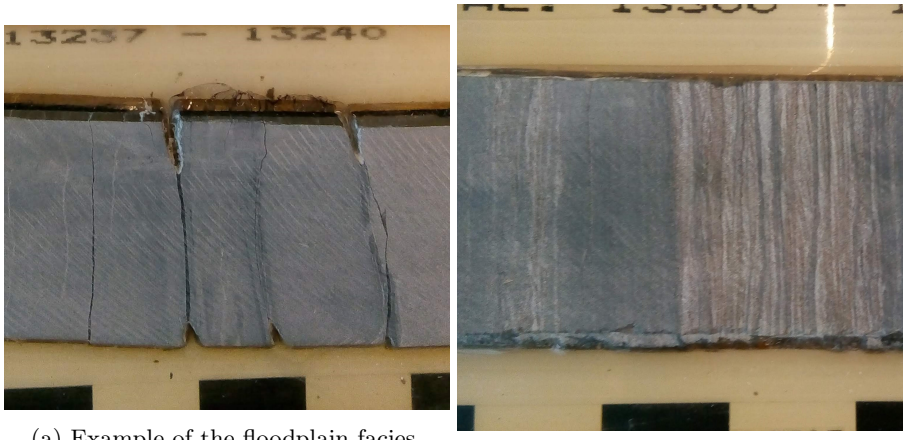

(a) Example of the floodplain facies.

(b) Example of the lacustrine facies.

Figure 7: Examples of the two shale facies present. The bars are 1/10 ft. long.

in contrast to the floodplain facies, does not indicate flow. This facies underlies a channel bar deposit, but since its bottom was not reached it is not known what it overlies. A photo of an example of this facies is included in figure 7b.

Swamp facies This facies is found in the core only once, and is very thin at about a half foot present in the core at 13264 ft. It consists of coaly shale. It has a flat laminated/layered structure in it and displays a coaly black colour. Because so little is present it is hard to determine the exact origin of the coal. However, it overlays a floodplain facies without marks of erosion. This makes it logical that it is part of floodplain vegetation. A floodplain in a braided river environment could contain a lot of static water, creating the anoxic conditions needed for the preservation of organic matter. If the river carries enough smaller grained material, the creation of swampy areas could be possible. A photo of an example of this facies is included in figure 8.

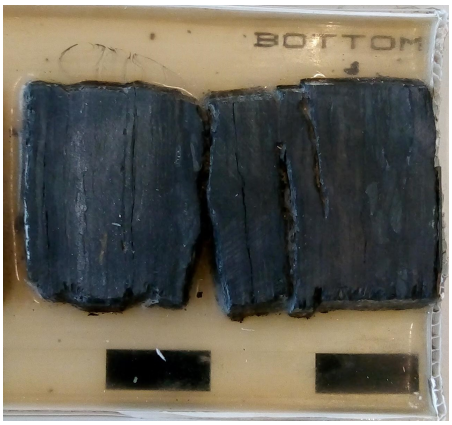

Figure 8: Photo of the coaly interval. Bars indicate 1/10 foot.

4.2 Well logs and core comparison

For the studied well, a complete set of downhole well logs was available. The results of this well logging are displayed in figure 9. This is before depth correction, so the cored interval in this picture is from 13216-13321 ft. This depth correlation is done from the peaks in the GR curve, which indicate the shale layers in the core. As we can clearly see, some features immediately stand out. These are the features we will be focusing on in the next sections.
The cored section starts with a section medium sands, as part of the channel bar facies, followed by a section of very coarse channel base sandstone. Unfortunately, the well logs do not show this difference, gamma ray is low, as with all sands, while the density is roughly constant at around 2.55 g/cm^3. The resistivity logs do show a slight difference, the medium resistivity is higher in the coarse sandstone. This is no conclusive indicator however as resistivity is more about the formation liquids than the formation itself. Then we have two peaks in gamma ray, with small increases in density, these two peaks are mostly due to increases in thorium and potassium content. They indicate the shales of the floodplain facies in the formation, which are rich in potassium minerals. The last feature from the well logs is a double peak, where the first peak coincides with a drop in density and an increase in neutron porosity as well as uranium content and travel times. The second peak looks like a normal shale of the floodplain facies, but the upper peak's depth corresponds well to the depth of a small coaly swamp facies. This makes sense because of the often relatively high levels of uranium present in organic matter. Also, the lower density of coal and other organic matter would explain the high travel times. (Crain, 1999)

4.3 Data analysis and PCA

The data from the well logs is very complete, giving good resolution. However, in order to use this data in a more handy way, we want to reduce its dimensionality. The well data comes in a 10-D data set, as each instrument can be seen to provide an extra data dimension. In order to make this more comprehensive and more easy to handle, we apply principal component analysis (PCA) to this data in order to reduce its dimensionality. This is done because PCA realignes the 10-D system axes along the axes of the smallest variance. This means that the first principal component axis in the PCA (PC1) shows the largest variance, and the last axis (PC10) the smallest. This can sometimes be used to compress large data sets into much smaller one, two or three dimensional data sets because it looks for common variability, which means that the last principal components can be neglected because they explain only a very small part of the variance.

If we apply PCA to our test interval (13205-13310 ft.), we need to firstly look at the explained variance per axis in order to validate if we can indeed used this.

As we can see in fig 10 and table 3, our first three components explain about 97.6% of the total variance, and our first two components explain about 88.9%. This means that we can quite accurately represent all of our data in PC1 and PC2.
However, feeding all the data into our analysis may create mistakes as some well logs are quite strongly correlated, and some may create an apparent change that is not relevant. This is the case in our logs for three instruments, depending on what we are analyzing. We will be focusing on identifying the coals and the coarse sand, so we split the results into two.

4.3.1 Swamp facies Results

In order to get relevant results for our coaly swamp facies, we firstly need to remove our total GR log. This is because the GR log measures the same as the compiled log of the thorium, potassium and uranium logs. Because this set of three logs is more informative than the one GR

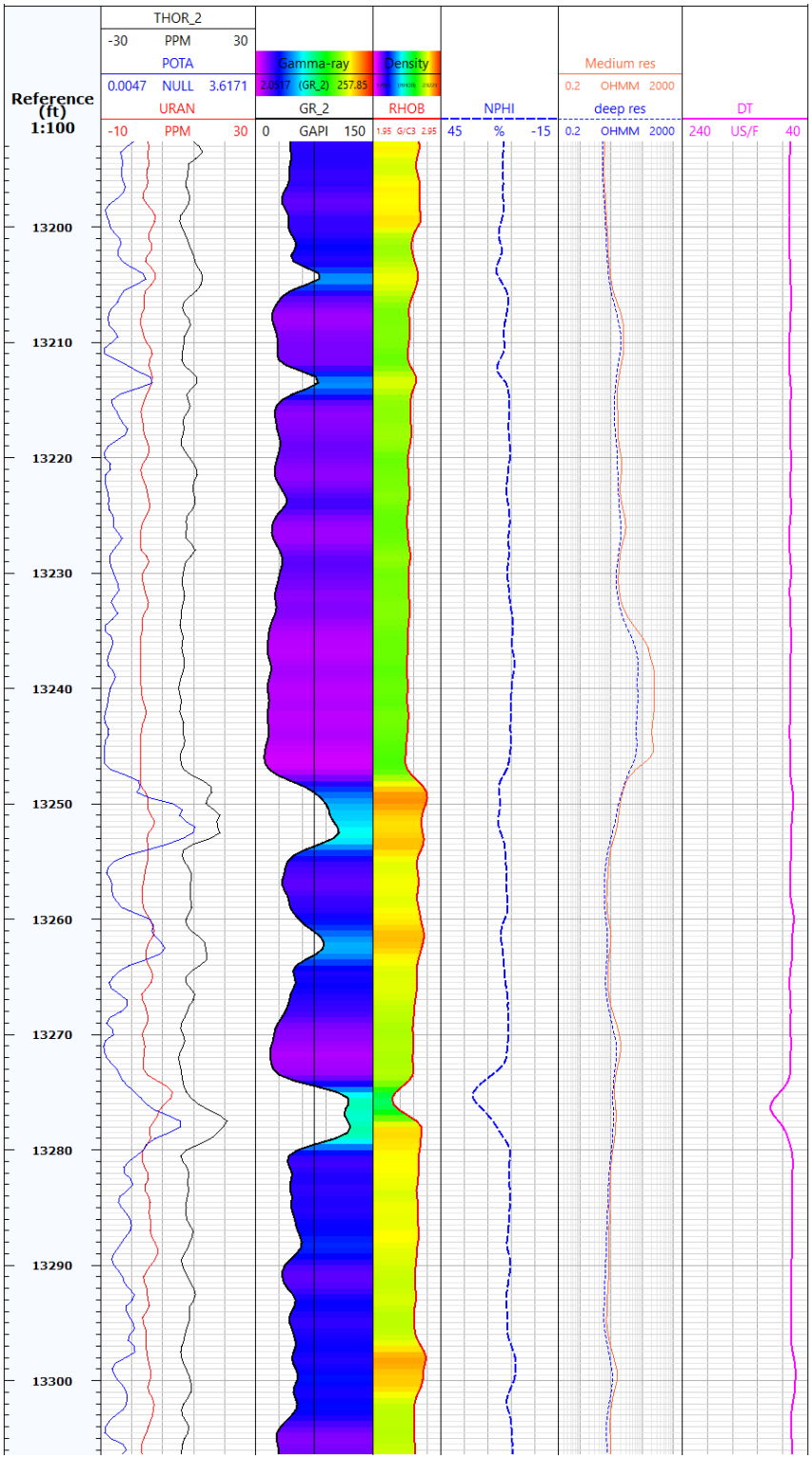

Figure 9: Well log suite for the cored interval. (13216-13321 ft. in this figure) (Oil and Gas Authority, 1996). For the meaning of the column headers see tables 1 and 2.

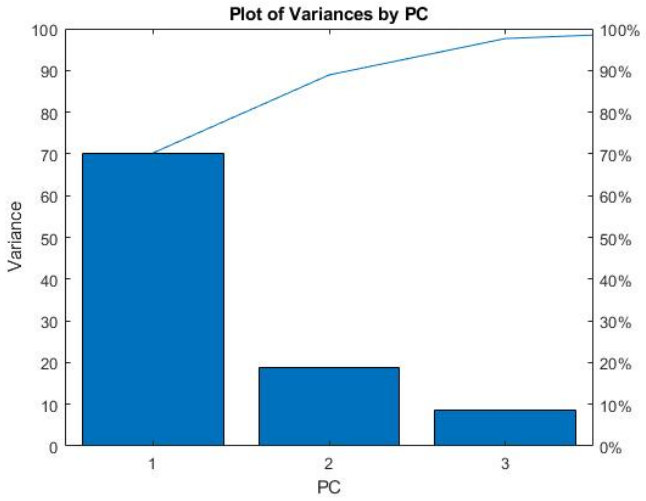

Figure 10: Explained variances per PC and cumulative variance explained

Principal Component	Explained Variance
PC1	70.2299
PC2	18.7043
PC3	8.7138
PC4	1.6645
PC5	0.4062
PC6	0.2444
PC7	0.0339
PC8	0.0021
PC9	0.0008
PC10	7.09e-05

Table 3: Explained variances per PC

log, we remove the GR log. Secondly, we remove the induction (ILD) log, because it is normally a mirror of the density (RHOB) log, so it will copy some of the variance. Thirdly, the tension log (TENS) is removed from the analysis, because it gives no relevant information about the actual formation. It increases with depth giving a skewed PCA. See also section 5.4.

If we remove the induction, tension and gamma ray logs as mentioned above, we get quite a different picture. As can be seen in table 4 and fig. 11. Now, PC1, PC2 and PC3 still explain almost all variance. From table 5 we can see how these principal components are actually build from the original data. As we can see, the most important logs for the variance in this data set are the sonic, neutron porosity and the thorium and uranium logs. We can now plot our scores in the PCA against depth to see what sort of variance is actually explained by which PC, as in figure 12.

If we compare this to our core data and our original well data, some features seem to correlate very well with some lithologies from our well log. Firstly, PC2 seems to show the shales that are present quite well, as it has three distinct peaks signifying the small shale layers present in the

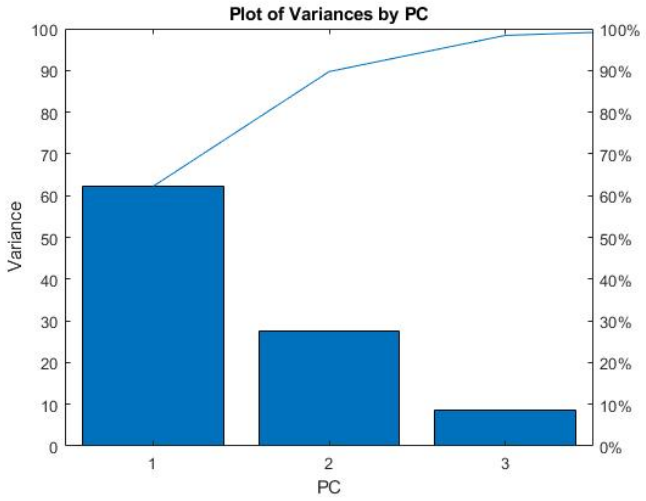

Figure 11: Explained variances per PC and cumulative variance explained for data edited for coal identification..

Principal Component	Explained Variance (%)
PC1	62.2
PC2	27.5
PC3	8.67
PC4	1.44
PC5	0.125
PC6	0.0349
PC7	0.00237

Table 4: Explained variances per PC in data edited for coal identification.

interval. It also shows that the lowest part scores significantly higher on PC2. However, some of these features are easier to spot on PC1. By adding PC1 and PC2 however, we get a very clear picture of our lithology, where the peaks are signifying the shale layers. We can see that the sands score significantly lower along this axis than the shales, as the sands almost all score negatively and and the shales are positive. Also, looking at PC3, we can see that the peak very well corresponds to the thin coaly layer in our interval. This is significant because it means that coals should be easily recognizable when this analysis is extended to other wells and intervals.

Log\PC	PC1	PC2	PC3	PC4	PC5	PC6	PC7
Caliper	0.0105	0.0122	0.0199	0.0494	0.112	0.971	-0.202
Sonic	0.724	-0.597	-0.34	0.0529	0.0215	0.00404	0.012
Neutron Porosity	0.537	0.2	0.731	-0.369	-0.0371	0.000356	0.00291
Potassium	0.0429	0.0805	0.0126	0.0315	0.984	-0.132	-0.0741
Density	-0.00258	0.0195	0.00563	0.0161	0.097	0.191	0.977
Thorium	0.405	0.769	-0.487	0.0488	-0.0761	0.00116	-0.00494
Uranium	0.15	0.0697	0.335	0.925	-0.0532	-0.0509	-0.00295

Table 5: Table of coefficients for the PCA, used in the analysis of coals.

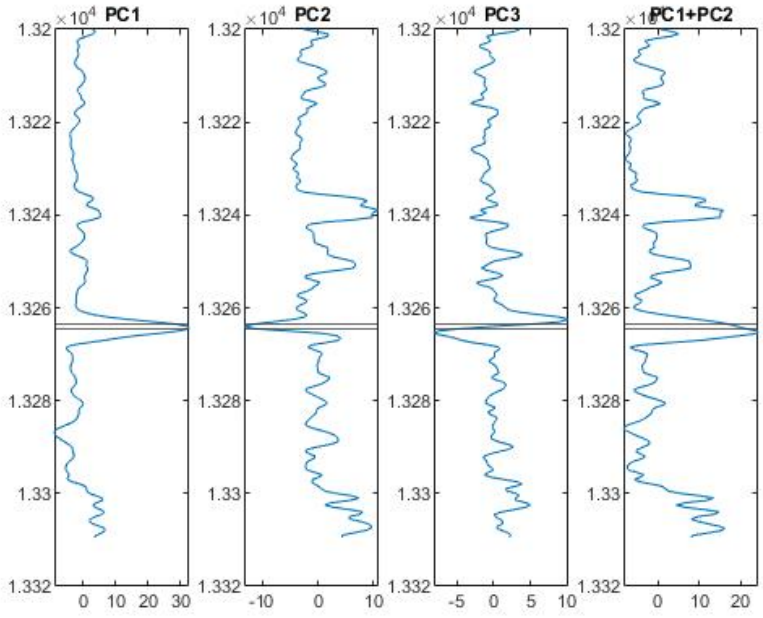

Figure 12: PC1-3 plotted against depth, giving a composite log. The lines in the plot indicate the real depth of the coal. Note how the PC3 log corresponds to the coal.

4.3.2 Channel Base Facies Results

The first step for the analysis of the channel base facies is quite similar for the swamp facies. In order to get relevant results for our Channel Base sands, the tension log (TENS) is removed from the analysis, because it gives no relevant information about the actual formation. It increases with depth giving a skewed PCA. However, if we do include the other logs, unlike the for the coals, we get different results.

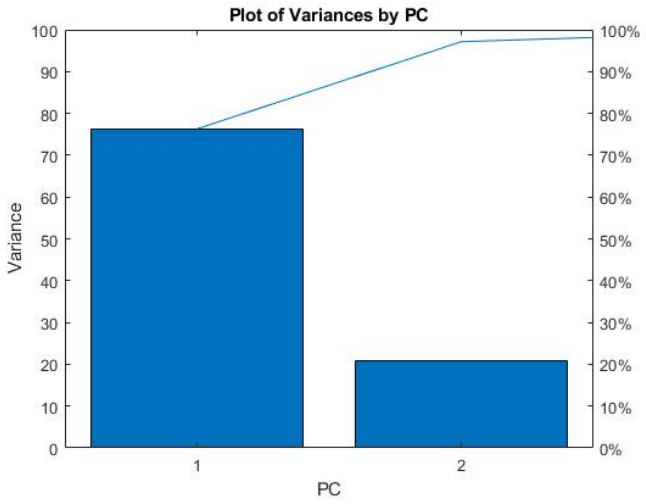

Figure 13: Explained variances per PC and cumulative variance explained for data edited for sands identification.

Principal Component	Explained Variance (%)
PC1	76.3
PC2	20.9
PC3	2.02
PC4	0.503
PC5	0.280
PC6	0.0388
PC7	0.0025
PC8	0.0011
PC9	8.66e-05

Table 6: Explained variances per PC in data edited for coarse sand identification.

As we can see from figure 13 and tables 6 and 7, this PCA gives very useful results since PC1 and PC2 combined explain more than 95% of the variance in this data package. This is good because that makes it very likely that if any variation is visible across the different sands, it will be visible in a combination of PC1 and PC2. In order to analyze this, we can plot the PC1 score and the PC2 score against each other, like was done in 14a. This plot shows 4 distinct point clouds. If we compare this to a the depth log of PC1 and PC2 in figure 14b, we can see that these point clouds correspond with the different sections in depth, and these in turn correspond to the lithology. It should especially be noted how the coarse sand section in the

Log\PC	PC1	PC2	PC3	PC4	PC5	PC6	PC7	PC8	PC9
Caliper	0.0038	-0.0034	0.0021	-0.0110	-0.0034	-0.0068	-0.1900	0.9700	-0.1300
Sonic	0.0440	0.0810	0.9400	0.1600	-0.3000	-0.0063	0.0100	0.0025	0.0120
Gamma Ray	0.9400	0.2800	-0.0880	-0.0910	-0.1100	-0.0470	-0.0210	-0.0087	-0.0033
Induction	-0.3000	0.9500	-0.0650	-0.0280	-0.0027	0.0042	-0.0017	0.0041	0.0003
Neutron Porosity	0.0920	0.0480	0.3200	-0.2000	0.9100	-0.1300	-0.0150	-0.0032	0.0030
Potassium	0.0140	0.0055	-0.0160	0.0210	0.0022	-0.1600	0.9700	0.1900	0.0080
Density	0.0018	-0.0012	-0.0140	0.0006	-0.0013	-0.0200	-0.0360	0.1300	0.9900
Thorium	0.1100	0.0540	-0.0860	0.9300	0.2600	0.2300	0.0120	0.0150	0.0015
Uranium	0.0370	0.0045	0.0620	-0.2500	0.0520	0.9500	0.1600	0.0380	0.0210

Table 7: Table of coefficients for the PCA, used in the analysis of sands.

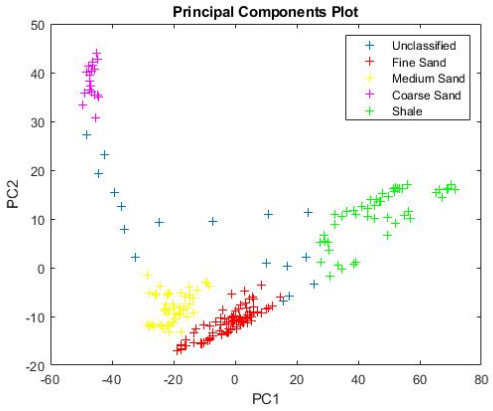

(a) Principal Component plot

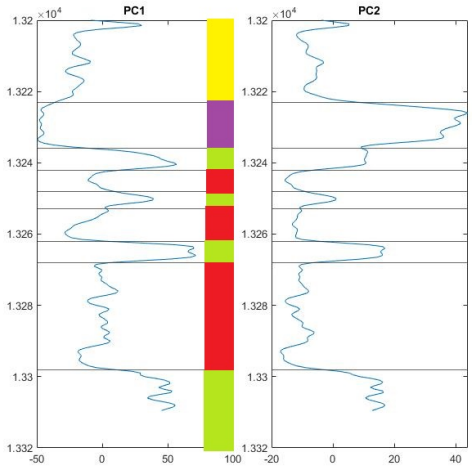

(b) Principal components against depth.

Figure 14: Principal component scores from coarse sand analysis plotted.

logs is now highlighted, as it scores very high on PC2, but very low on PC1. This means we can now distinguish between these two sands, something that was impossible from the original data. We can also see that there is a distinction between the two sands from the Channel Bar facies, although they it is less distinct. The points indicating the different shale facies are also separated, but they are somewhat less grouped.

4.4 Extrapolation in the Well

From the results from the previous section we can start to find these facies in the rest of the well. For now, we only try to extrapolate the Swamp facies and the Channel Base facies because they are targets that are very distinct, and are interesting targets for future research. The fact they are rather distinct is necessary, because our data set is relatively small and therefore it will not include all the variation that will be visible over the whole of the well and even more so the variance that is visible in other wells. Since the coals and the very coarse sand have a rather distinct signature and are specific targets, the variation within their groups is probably smaller.

For example, there are many more sandstone variants than there are coals in this well. The results are displayed in figure 15.
This is done as described in section 3.6, which means that the well data are firstly formatted according to the specifications from section 3.4. The mean of the well data over the cored interval is then subtracted and the columns of well data are multiplied with the coefficients matrices in figures 5 and 7 for the Swamp and Channel Base facies respectively. This data is then used in the classification.

4.4.1 Swamp Facies Extrapolation

In order to identify the coals that are present in the rest of the well, a script has been written. This script is in appendix D. If we run this over the rest of the formation, excluding the Zechstein formation, since it can not really be interpreted in terms of the cored interval, so from 12800 to 13800 ft., we find the coals to be present in many places. The exact locations are shown in table 8a. However, this data was not corrected for depth, as was done with the data from the cored section, so this still needs to be done. We can see that there are 40 coals present according to this script in the measured interval. If we check this against the core photos, we of course find the Swamp facies that was cored at 13263.5 ft. However, core photos are also available from a core that was taken from 12795 to 12865 ft. We can check our method against these photos to enable us to say something about the accuracy of the method. Only one coal was detected in that interval, at 12831 ft. Looking at the core photos, this looks to be correct. The core photos look to show a coaly shale starting at 12832 ft., which could be correctly identified by the method, although the depth is slightly off.
However, the well report (Samway & Goodall, 1992) identifies 18 coals in the interval which was sampled. Since we find 40, it might look like something has gone wrong. However, the well report does not include the thin Swamp facies coal in our cored interval. This is shown in appendix B.The good thing is that all the 18 coals in the report were also identified in the script, for as far as can be traced. So the accuracy of the method is good, giving 40 results, of which 19 can be confirmed as correct. (18 from report, 1 from core). That does not mean that the rest is incorrect, but more that those cannot currently be determined to be correct.

4.4.2 Channel Base Facies Extrapolation

For the Channel Base facies, our results take the same shape, they are displayed in table 8b. As we can see, we only found the Channel Base sand that was in our test data. According to this method, this section is thus the only such sections in the well. Since no other coarse sands could be seen in the core photos, we cannot say much about the accuracy of the method from that. The well report from Samway & Goodall (1992) does however reveal that some channel fill deposits are present in the interval, although their exact grain size could not directly be inferred from this. It is very likely however, that other coarse intervals are present, but they remain undetected.

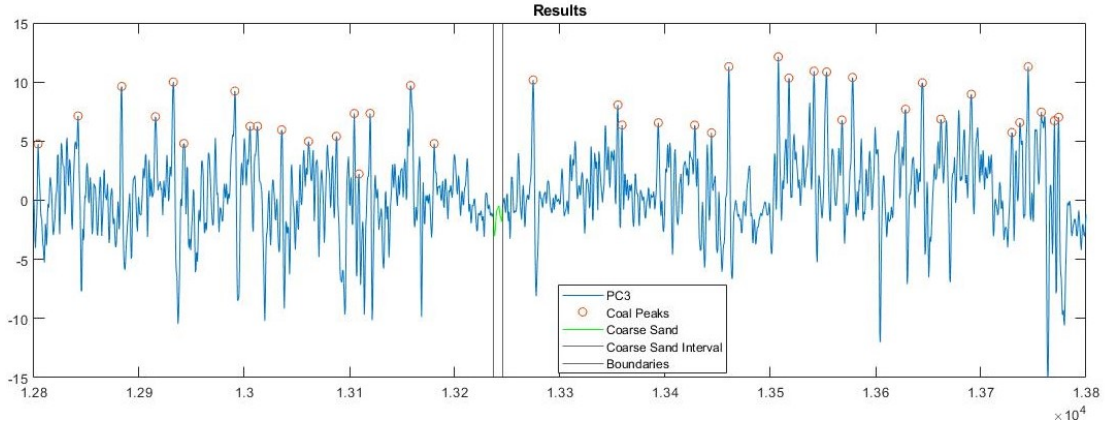

Figure 15: Comprehensive Log Chart of the results based on the Coal PC3 log.

Coal Depths (ft.)	Coal Corrected Depths (ft.)
12804	12793
12842	12831
12883.5	12872.5
12915.5	12904.5
12932.5	12921.5
12942.5	12931.5
12991	12980
13005.5	12994.5
13012.5	13001.5
13035.5	13024.5
13061	13050
13087.5	13076.5
13104.5	13093.5
13109	13098
13119.5	13108.5
13158	13147
13180.5	13169.5
13274.5	13263.5
13355	13344
13359	13348
13393.5	13382.5
13428	13417
13444	13433
13460.5	13449.5
13507.5	13496.5
13517.5	13506.5
13541.5	13530.5
13553.5	13542.5
13568	13557
13578	13567
13628.5	13617.5
13644.5	13633.5
13662	13651
13691	13680
13729.5	13718.5
13737	13726
13745	13734
13757.5	13746.5
13770	13759
13774	13763

(a) Depths of Coal Layers in Data and Corrected Depths.

Coarse Sand Depth Raw (ft.)	Coarse Sand Corrected Depths (ft.)
13236.5	13225.5
13237	13226
13237.5	13226.5
13238	13227
13238.5	13227.5
13239	13228
13239.5	13228.5
13240	13229
13240.5	13229.5
13241	13230
13241.5	13230.5
13242	13231
13242.5	13231.5
13243	13232
13243.5	13232.5
13244	13233
13244.5	13233.5
13245	13234
13245.5	13234.5

(b) Depths of Coarse Sand layer in Data and Corrected Depths.

5 Discussion

Here we will discuss the results from the previous section. We will go over all the results from the last section and try to identify errors and inaccuracies as well as making suggestions for further research where appropriate.

5.1 Core Logging & Interpretation

The core logging part of this project is quite straight forward. The biggest problem here, and one of the biggest problems overall is that there is not a lot of core material. Although roughly 100 feet of core has been studied, the total length of the well is more than 15000 ft. although not the complete well was relevant. In total, about a 1000 feet was used to find the coals and the coarse sand from. So it is no surprise that not all the rocks are present in the core. That said, the actual well logging method as used in this thesis (systematic and detailed description, even on small scale) is nothing unusual. (Blackbourn, 2012) The danger with this method is that medium scale structures (dm scale) might be missed because the focus is so much on smaller scales. Another problem with this core was that quite some pieces were missing, be it smaller samples used for different tests or entire three foot slabs of core, with the latter being a much bigger problem. Because of this last problem, the layer boundary between the last long layer of shale and the sandstone above was not present. Although core photos were present, they were of such quality that small scale structures such as lamination could not be distinguished clearly from them. Some more detailed study into the missing parts of the core could be helpful in the future. Lastly, the interpreter of the facies did not have much experience with the carboniferous rocks which presented themselves during the study. As such, interpretations might be wrong. The most likely candidates for this are the Lacustrine facies and the Swamp facies. In case of the Lacustrine facies, other explanations could also fit.
However, if we look at the work from O'Mara (1995), who has already done work on facies in this environment, we see that the Lacustrine facies in this report correspond very well to what is described there as Lake Margin facies. According to O'Mara (1995), 'Well laminated grey claystone and siltstone, with occasional thin sandstones characterise this facies', which fits the description very well. A similar conclusion can also be drawn on the Swamp facies, although they also bear some similarities to what in O'Mara (1995) is described as Coal-bearing alluvial plain facies. It seems that the other facies described in this report do not have equivalents in his work though.
However, in the report by Samway & Goodall (1992), the facies are also described, be it in less detail. This report does also interpret the exact core interval, but in less detail. (See appendix B) However, that interpretation does correlate quite well with the work in this report. According to Samway & Goodall (1992), the interval has 3 instead of four shales, the one ft thick shale of the Floodplain facies was not described. They also group the sandstones differently, not by facies but by gamma ray response. It does show however the channel fill origin of the sandstones meaning that our interpretation is probably correct. If we look at the alluvial plain facies we defined, they are very similar to what is defined in the well report. The same goes lacustrine facies which is, according to Samway & Goodall (1992), indeed of lacustrine origin, although it indicates that could also have a bay origin, instead of a lake. This is interesting as O'Mara (1995) would interpret this facies more as a lake margin environment, but the difference between the two is minor, meaning that our interpretation of the facies being lacustrine is probably correct or very close. The figures from Samway & Goodall (1992) which indicate these things are present in appendix B.

5.2 Well logs

As for the well logs, we can assume they are accurate since they were taken by a company that has made these measurements it business. So the data itself is very probably correct. If there are any errors, they are in interpretation and the method of interpretation and data usage. The first data interpretation in this and other cases is often done without computers by just eyeing it. This is good as it gives a first indication of what to expect over the interval. However, this is a skill that is normally perfected with experience, which the author of this thesis does not have. This first interpretation was thus done based on basic principles of well logging, for example the idea that high GR scores often mean the presence of shales. However experts in the field can often recognize patterns in the data that could indicate otherwise. This is a skill that builds with experience.

5.3 Core/Well Logs Correlation

As with the well logs, the comparison between the core and the well logs was done by hand. As it is known that in general shales generate high gamma ray peaks, they can be easily compared to the well log. Further calibration was done using the coal layer, which has a particular uranium signature. This means that the correlation between the two is well grounded and can be assumed correct. Although it would be interesting to further investigate the response from the coal layer, as although it can be recognized through a combination of its uranium and sonic signature, these peaks do not completely line up and thus can give problems in classifying them using computers. If this is because of distances between the different tools on the wireline, it should be easily solved, but if other factors are at play, this could increase the accuracy of the extension of these layers further on. This correlation is mostly confirmed by Samway & Goodall (1992).

5.4 Data analysis and PCA

In section 4.3 we looked at the results data analysis and the PCA. As mentioned there, not all data was included in the PCA because it skewed the result. The tension, gamma ray and induction logs were left out. This is because they either measured something that was not relevant, like the tension logs, or inputting them would be inputting signals twice, like with the gamma ray and the induction log. However, instead of leaving the last two out, we could have also kept out the logs they mirror. This would however mean that some vital information would have been left out as well. As we can see in table 5, the different gamma ray logs have very different coefficients in order to highlight different features in the data. This information would be lost if we used the GR log instead. And this matters, because PC3, from which the coals are very clearly visible, relies heavily on this information. For the induction log this is different. Density is only really important for PC7, which only explains only a very small portion of the variance, as seen in table 4. Also in section 4.3 it is stated that adding PC1 and PC2 give a very good idea of the lithology and that PC3 clearly indicates the coaly Swamp facies interval. This might be correct, but since it was assessed mostly by estimation, a good statistical analysis of how strongly these features correspond would be recommended for future research.
In the last paragraph we discussed how leaving out the induction and density logs was very important to make the coals recognizable. However, this is not the case for the coarse Channel Base sands. It only became visible in the analysis after only taking out the tension log, although there may be more combinations that would show the coarse sand. As there are many possible combinations, not all were tested. However, looking at table 7, it is likely that the induction log result is the reason for this, as the density log is not a major factor in either of the two principal component axes. This is a strange phenomenon and it is not clear where this is coming

from. Since resistivity has components both from the formation as well as from the formation fluids, it cannot be for sure that this result is valid, since the formation fluids are not part of the properties of a layer. High resistivity in formation fluids can for example be caused by the presence of gas in the pore space, which is a possibility since this well was drilled as part of a gas exploration operation. However, it is also possible that this coarse sandstone for some reason is less conductive than normal and that this result is therefore valid. More research into this result is highly recommended.

5.5 Well Facies Extrapolation

In order to extend these layers over the rest of the well we used the script in appendix D. Although the script was written by the author, its big downfall is in the short cored section. This project is somewhat based on the assumption that all variability within a facies is encountered in the core, but this is of course not the case. As also explained in the last paragraph, the detection of the Channel Base facies leans strongly on the induction values of that sand (see table 7) which does not necessary mirror a property of that sand. Also, the well report does indicate that some coarse sections of coarse channel fill deposits were present, which were not detected. It also indicates the cored Channel Base facies as being a potential reservoir, making it even more likely that the detection method used was based reacted to the presence of some amount of gas in the pore space. The figures from Samway & Goodall (1992) are present in appendix B.
As such, the detection of coals is probably much more accurate. Although it is based on only a very thin layer of coal, this layer does have a strong signature in the well logs and the principal components. The shortfall in this analysis is that the script only picks up the peaks with a certain prominence, which was based on trying out what peak prominence would only give one detection on the cored interval in the right location and is thus somewhat arbitrary since there are more values that work. Thus, smaller peaks that are not clearly visible on the well logs but could signify coals could be left undetected, although a conservative setting on the peak prominence does reduce the chances of that. Other problems in the detection of coals is that since only peaks are detected, the thickness of the coal is not directly apparent and can only be determined by closer examination. This is a shortfall in the detection method. Lastly, the detected depths of the peaks is not exactly the correct depth, some deviation is present. This can be seen by comparing the results from table 8a to a plot of the well logs. The peak in the third principal component (PC3) occurs at 13263.5 ft., where in reality the coal is a bit further down at 13264 ft. The same goes for many of the other results, if they are compared to the logs in appendix A, the spikes in sonic log (note: not all peaks in sonic represent coals) which signify the coals do not always completely line up with the results from table 8a, but can be a few feet off. This is a downside but it is not major.
Also, we have tried to use the core photos as verification, as explained in section 4.4.1, but this has not been as succesful as hoped. Since only 1 coaly Swamp facies interval was detected in that cored interval (12795 to 12865 ft.), very little possibility for verification was provided. The detection at 12831 ft. is probably correct though, but it cannot be said for sure. The core photos are of poor quality, but it looks like some coal is present around that depth, although not exactly at that depth. However, a total of 18 coals could be confirmed from the report by Samway & Goodall (1992). This means that 21 of our 40 detected coals and thus 21 of the 40 Swampy facies are not confirmed. There is however good reason to think that at least some of them are correct. We know that our Swamp facies is present at a depth of 13264 ft. from the core, but it is not present in the aformentioned report. Since we know it is there, it is likely that there are quite a few shaley coals, judging from the fact that the 40 we detected are not all included in the well stratigraphy as given by Samway & Goodall (1992) in appendix B. Our method probably picks

up on shaly coals as well as normal coals as that was what is was designed around, which the well report does not.
Overall the results achieved in this thesis are quite satisfactory, as many layers can be recognized in the rest of the well and this method can without trouble be expanded to fit different wells as well. It would also be interesting to expand the path taken in recognizing the coarse sand as set out in section 3.5 and executed in section 4.2 to classify lithologies based on their signature in the principal component analysis, as only based on this core we can already see a difference between two sands. By expanding the PCA and the control data set, this method could be used to differentiate sands with different properties quite easily.

References

Blackbourn, G. A. (2012). *Cores and core logging for geoscientists* (2nd ed.). Whittles Publishing. Retrieved from https://www.ebook.de/de/product/24834400/graham_a_blackbourn_cores_and_core_logging_for_geoscientists.html

Cameron, D., Munns, J., & Stoker, S. (2005). Remaining hydrocarbon exploration potential of the carboniferous fairway, uk southern north sea.

Collinson, J., Jones, C., Blackbourn, G., Besly, B., Archard, G., & McMahon, A. (1993). Carboniferous depositional systems of the southern north sea. In *Geological society, london, petroleum geology conference series* (Vol. 4, pp. 677–687).

Crain, E. (1999). *Crain's petrophysical handbook.* Retrieved from https://www.spec2000.net/index.htm

Guion, P., & Fielding, C. (1988). Westphalian a and b sedimentation in the pennine basin, uk. In B. Besly & G. Kelling (Eds.), *Sedimentation in a synorogenic basin complex. the upper carboniferous of northwest europe* (p. 153-177). London: Blackie.

Hampson, G., Davies, S., Elliott, T., Flint, S., & Stollhofen, H. (1999). Incised valley fill sandstone bodies in upper carboniferous fluvio–deltaic strata: recognition and reservoir characterization of southern north sea analogues. In *Geological society, london, petroleum geology conference series* (Vol. 5, pp. 771–788).

Huang, B., Xu, R., Fu, C., Wang, Y., & Wang, L. (2018). Thief zone assessment in sandstone reservoirs based on multi-layer weighted principal component analysis. *Energies*, *11*(5), 1274.

Leeder, M. R., & Hardman, M. (1990). Carboniferous geology of the southern north sea basin and controls on hydrocarbon prospectivity. *Geological Society, London, Special Publications*, *55*(1), 87–105.

Nichols, G. (2009). *Sedimentology and stratigraphy.* John Wiley & Sons.

Oil and Gas Authority. (1996). *Uk national data repository.* Retrieved from https://ndr.ogauthority.co.uk/

O'Mara, P. T. (1995). *Correlation, facies distribution and sequence stratigraphic analysis of the westphalian b coal measures in quadrant 44 of the southern north sea* (Unpublished master's thesis).

O'Mara, P. T., & Turner, B. R. (1997). Westphalian b marine bands and their subsurface recognition using gamma-ray spectrometry. *Proceedings of the Yorkshire Geological Society*, *51*(4), 307–316.

Rider, M. (1990). Gamma-ray log shape used as a facies indicator: critical analysis of an oversimplified methodology. *Geological Society, London, Special Publications*, *48*(1), 27–37.

Samway, G., & Goodall, I. (1992). *A sedimentological, petrographical and reservoir quality evaluation of the drilled rotliegend (permian) and westphalian a to b (carboniferous) intervals in well 44/21a-6, and a comparison with similar intervals in other 44/21a prospect wells, southern north sea, ukcs.* [techreport]. Retrieved 2020-04-07, from https://ndr.ogauthority.co.uk/.

van den Berg, S., J.H.; Nio. (2010). *Sedimentary structures and their relation to bedforms and flow conditions.* European Association of Geoscientists & Engineers (EAGE). Retrieved 2020-02-25, from https://app.knovel.com/hotlink/toc/id:kpSSTRBFC1/sedimentary-structures/sedimentary-structures doi: 10.3997/9789462820180

Wolf, K. (1999). *Introduction to the physics of rocks: Theory and applications.*

A Well logging Suite over a longer interval

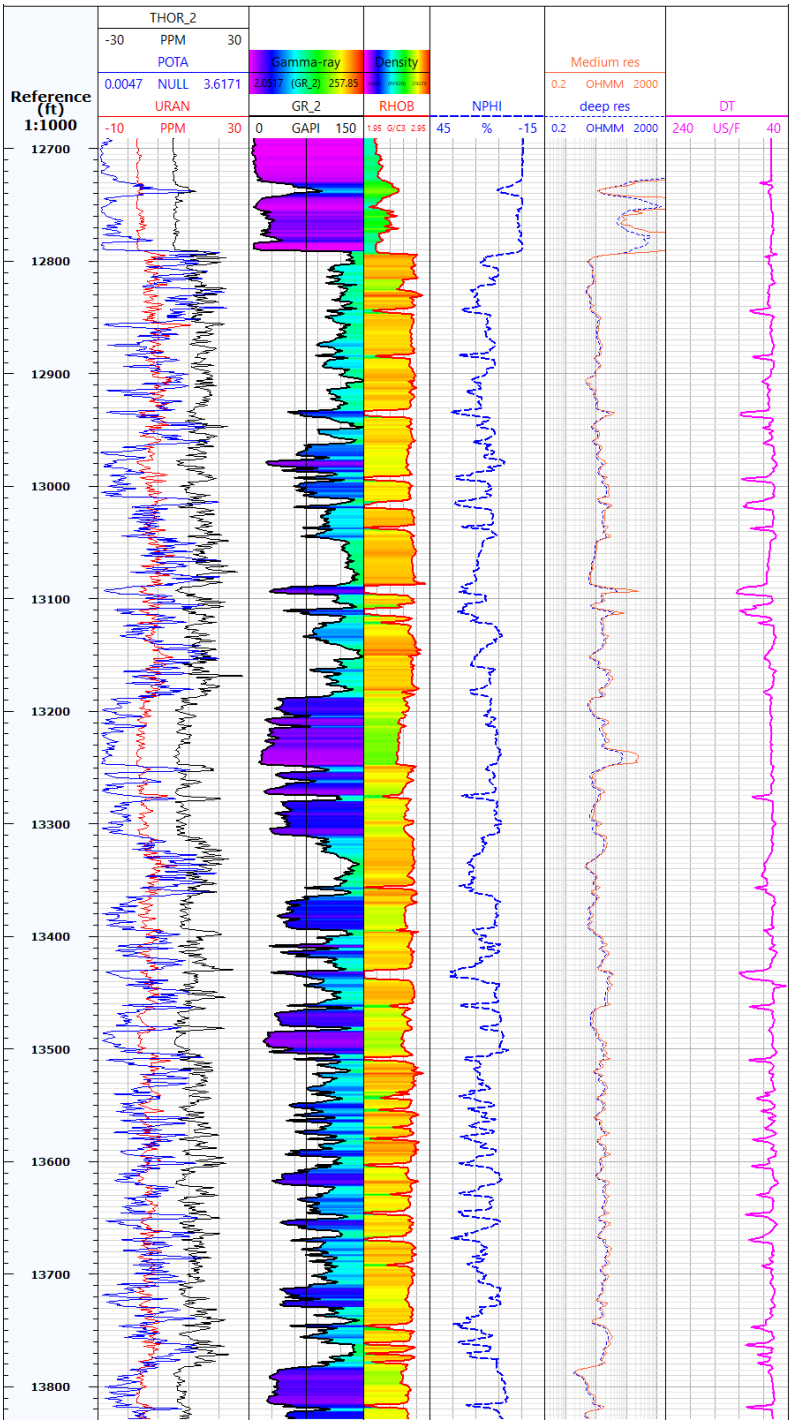

B Interpretations from drilling geologist

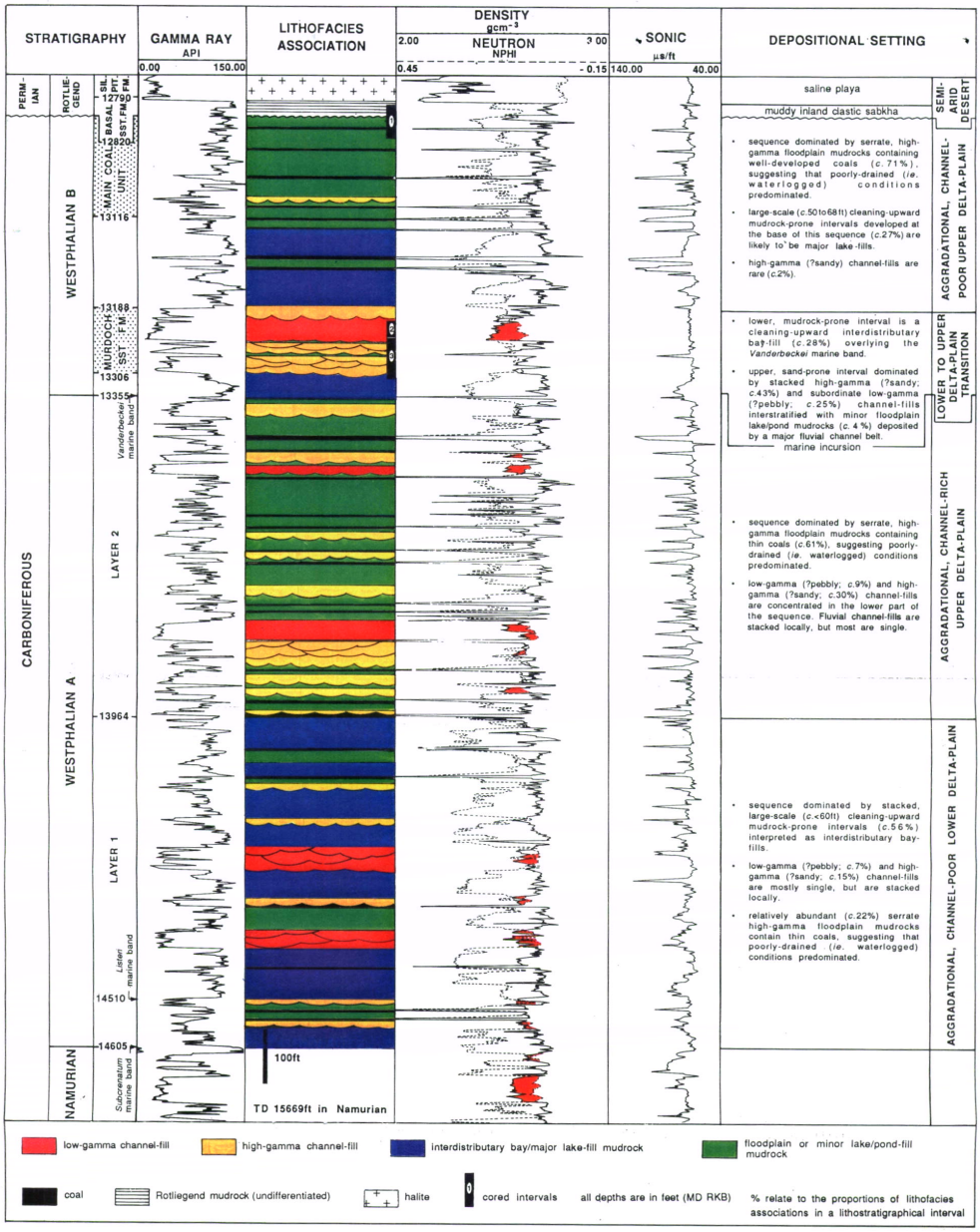

Figure 16: Well Stratigraphic overview and interpretation. (Samway & Goodall, 1992).

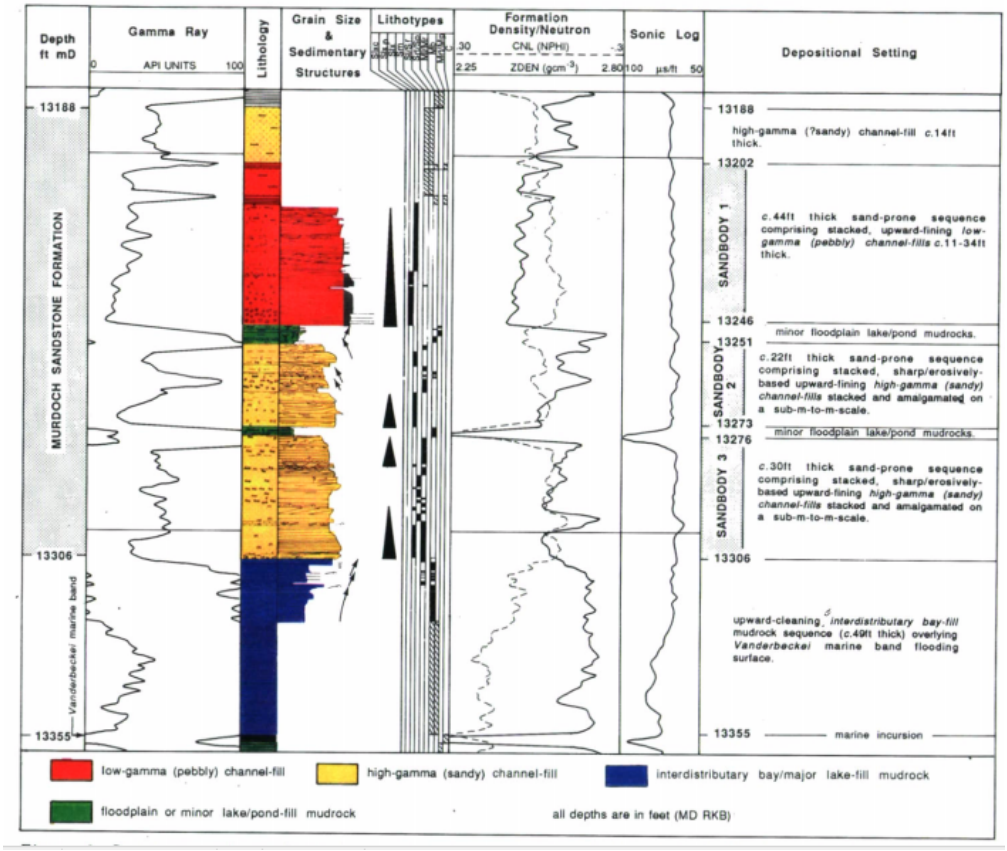

Figure 17: Interpretation of the cored well interval studied in this report as done by Samway & Goodall (1992).

.

C MatLab script for initial analysis of cored interval

Please note that this script is not completely up to date, as it is a file in working condition, including material from what turned out to be a dead end.

```
close all

%% Import data from spreadsheet
% Script for importing data from the following spreadsheet:
%
%    Workbook: C:\Users\rutger\Documents\TU\BEP\Log Data\Raw Data_Interval.xlsx
%    Worksheet: Well_44_21a-_6_jwl_JWL_FILE_168
%
% To extend the code for use with different selected data or a different
% spreadsheet, generate a function instead of a script.

% Auto-generated by MATLAB on 2020/03/04 14:58:54

%% Import the data
[~, ~, raw] = xlsread('C:\Users\******\Raw Data_Interval.xlsx','Well_44_21a-_6_jwl_JWL_FILE_168','A2:K221'

%% Create output variable
data = reshape([raw{:}],size(raw));

%% Create table
RawDataInterval = table;

%% Allocate imported array to column variable names
RawDataInterval.DEPT = data(:,1);
RawDataInterval.CALI = data(:,2);
RawDataInterval.DT = data(:,3);
RawDataInterval.GR = data(:,4);
RawDataInterval.ILD = data(:,5);
RawDataInterval.NPHI = data(:,6);
RawDataInterval.POTA = data(:,7);
RawDataInterval.RHOB = data(:,8);
RawDataInterval.TENS = data(:,9);
RawDataInterval.THOR = data(:,10);
RawDataInterval.URAN = data(:,11);

%% Clear temporary variables
clearvars data raw;
%% Convert data and pca

henk=table2array(RawDataInterval);
Henk=henk(:,[2 3 4 5 6 7 8 10 11]);

[coeff, score, latend, tsd, variance] = pca(Henk);

%% Scree Plot

figure
plot(variance) %%Pareto(variance) also gives very useful results
title('Plot of Variances by PC')
xlabel('PC')
ylabel('Variance')

%% Pareto
figure
pareto(variance)
```

```
title('Plot of Variances by PC')
xlabel('PC')
ylabel('Variance')

%% Plot Components

figure()
plot(score(:,1),score(:,2),'+')
xlabel('PC1')
ylabel('PC2')
title('Principal Components Plot')

%% 3D Plot

figure()
biplot(coeff(:,1:3),'Scores',score(:,1:3));
axis([-.26 0.8 -.51 .51 -.61 .81]);
view([30 40]);

%% Export Data
%writematrix(score,'PCdata.xlsx','Sheet',1,'Range','B2:K221');

%% Plot Data

tiledlayout(1,2,'TileSpacing','none');

nexttile
plot(score(:,1),RawDataInterval.DEPT)
yline(13223)
yline(13236)
yline(13242)
yline(13248)
yline(13253)
yline(13262)
yline(13268)
yline(13298)
title('PC1')
set(gca,'Ydir','reverse')

nexttile
plot(score(:,2),RawDataInterval.DEPT)
yline(13223)
yline(13236)
yline(13242)
yline(13248)
yline(13253)
yline(13262)
yline(13268)
yline(13298)
title('PC2')
set(gca,'Ydir','reverse')

% nexttile
% plot(score(:,3),RawDataInterval.DEPT)
% yline(13264.5)
% yline(13263.5)
% title('PC3')
% set(gca,'Ydir','reverse')
%
% nexttile
% plot(score(:,2)+score(:,1),RawDataInterval.DEPT)
% yline(13264.5)
```

```
% yline(13263.5)
% title('PC1+PC2')
% set(gca,'Ydir','reverse')


%See: https://nl.mathworks.com/help/stats/quality-of-life-in-u-s-cities.html

%% Check Data
figure()
plot(score(:,1),score(:,2),'+')
hold on
xlabel('PC1')
ylabel('PC2')
title('Principal Components Plot')

A=size(score);
LithoEmpty=zeros(A(1,1),1);
LithoLog=[score LithoEmpty];

% PC3=score(:,3);
% [PC3pks,PC3locs,PC3w,PC3p] = findpeaks(PC3,'MinPeakProminence',8);
% Coalpks=RawDataInterval.DEPT(PC3locs);



for s=1:A(1,1)
    if ((((score(s,2)+12)-(4/7)*(score(s,1)+2))^2)/(8^2*(1+(4/7)^2)))+((((4/7)*(score(s,2)+12)+(score(s,1)
      LithoLog(s,end)=1;
    elseif (((score(s,1)+20)^2)/12^2)+(((score(s,2)+5)^2)/12^2)<=1
        LithoLog(s,end)=2;
    elseif ((((score(s,2)-36.5)-(-19/13)*(score(s,1)+46.5))^2)/(8^2*(1+(-19/13)^2)))+((((-19/13)*(score(s,
        LithoLog(s,end)=3;
    elseif ((((score(s,2)-9.9375)-(59/128)*(score(s,1)-48))^2)/(10^2*(1+(59/128)^2)))+((((59/128)*(score(s
        LithoLog(s,end)=4;
    end
end

% for s=1:A(1,1)
%     ind(1,1)=((((score(s,2)+12)-(4/7)*(score(s,1)-0.75))^2)/(8^2*(1+(4/7)^2)))+((((4/7)*(score(s,2)+12)+
%     ind(2,1)=(((score(s,1)+22)^2)/11^2)+(((score(s,2)+5)^2)/11^2);
%     ind(3,1)=((((score(s,2)-36.5)-(-19/13)*(score(s,1)+46.5))^2)/(8^2*(1+(-19/13)^2)))+((((-19/13)*(scor
%     ind(4,1)=((((score(s,2)-9.9375)-(59/128)*(score(s,1)-48))^2)/(10^2*(1+(59/128)^2)))+((((59/128)*(sco
%     [NU, match]=min(ind);
%     LithoLog(s,end)=match;
% end

index1=find(LithoLog(:,end)==1);
plot(score(index1,1),score(index1,2),'+','Color',[1 0 0])

index2=find(LithoLog(:,end)==2);
plot(score(index2,1),score(index2,2),'+','Color','yellow');

index3=find(LithoLog(:,end)==3);
plot(score(index3,1),score(index3,2),'+','Color','magenta');

index4=find(LithoLog(:,end)==4);
plot(score(index4,1),score(index4,2),'+','Color','green');



%% Lithology plots
```

```
figure()
hold on
plot(score(index1,1),henk(index1,1),'Color',[1 0 0])
plot(score(index2,1),henk(index2,1),'Color','yellow');
plot(score(index3,1),henk(index3,1),'Color','magenta');
plot(score(index4,1),henk(index4,1),'Color','green');
set(gca,'Ydir','reverse')

figure()
hold on
plot(score(index1,2),henk(index1,1),'Color',[1 0 0])
plot(score(index2,2),henk(index2,1),'Color','yellow');
plot(score(index3,2),henk(index3,1),'Color','magenta');
plot(score(index4,2),henk(index4,1),'Color','green');
set(gca,'Ydir','reverse')
```

D MatLab script for well extension

This script can be used by matlab, but the data locations will have to be formatted to fit different computers of course.

```
% Script for finding the Coals and the coarse sand intervals present in
% the well.

%% Import the data
[~, ~, raw] = xlsread('C:\Users\********\Raw Data_Interval.xlsx','Well_44_21a-_6_jwl_JWL_FILE_168','A2:K22

%% Create output variable
data = reshape([raw{:}],size(raw));

%% Create table
RawDataInterval = table;

%% Allocate imported array to column variable names
RawDataInterval.DEPT = data(:,1);
RawDataInterval.CALI = data(:,2);
RawDataInterval.DT = data(:,3);
RawDataInterval.GR = data(:,4);
RawDataInterval.ILD = data(:,5);
RawDataInterval.NPHI = data(:,6);
RawDataInterval.POTA = data(:,7);
RawDataInterval.RHOB = data(:,8);
RawDataInterval.TENS = data(:,9);
RawDataInterval.THOR = data(:,10);
RawDataInterval.URAN = data(:,11);

%% Clear temporary variables
clearvars data raw; % Auto-generated by MATLAB on 2020/03/04 14:58:54
%% Convert data and pca for the Coals.

henk=table2array(RawDataInterval);
CoalSet=henk(:,[2 3 6 7 8 10 11]);

[coeffC, scoreC, latendC, tsdC, varianceC] = pca(CoalSet);

%% Convert data and pca for the Sands.

SandSet=henk(:,[2 3 4 5 6 7 8 10 11]);

[coeffS, scoreS, latendS, tsdS, varianceS] = pca(SandSet);

%% Check Data
A=size(scoreC);
LithoEmpty=zeros(A(1,1),1);
LithoLog=[scoreC LithoEmpty];

PC3=scoreC(:,3);
[PC3pks,PC3locs,PC3w,PC3p] = findpeaks(PC3,'MinPeakProminence',10);
Coalpks=RawDataInterval.DEPT(PC3locs);



%% Setup the Import Options and import the data
opts = spreadsheetImportOptions("NumVariables", 11);

% Specify sheet and range
```

```
opts.Sheet = "Well_44_21a-_6_jwl_JWL_FILE_168";
opts.DataRange = "A1871:K7574";

% Specify column names and types
opts.VariableNames = ["DEPT", "CALI", "DT", "GR", "ILD", "NPHI", "POTA", "RHOB", "TENS", "THOR", "URAN"];
opts.VariableTypes = ["double", "double", "double", "double", "double", "double", "double", "double", "dou

% Import the data
a6petrophysicaldatarawEDITED = readtable("C:\Users\********\Log Data\44_21a-6_petrophysical_data_raw_EDITE

%% Clear temporary variables
clear opts % Auto-generated by MATLAB on 18-Mar-2020 11:27:07

%% Load and select data

honk=table2array(a6petrophysicaldatarawEDITED);
FullCoalSet=honk(:,[2 3 6 7 8 10 11]);

%% Build depth array

indupper=find(honk(:,1)==12800);
indlower=find(honk(:,1)==13800);
Depth=honk(:,1);
DepthInterval=Depth(indupper:indlower,:);

CoalLogDataArray=FullCoalSet(indupper:indlower,:);

%% Applying PCA to well data for Coals.

PCDatC = bsxfun(@minus,CoalLogDataArray,mean(CoalSet));
PCADataArrayCoal=mtimes(PCDatC,coeffC);

%% PCA Data Analysis for Coals.
PC3DataC=PCADataArrayCoal(:,3);
[D3pks,D3locs,D3w,D3p] = findpeaks(PC3DataC,DepthInterval,'MinPeakProminence',8);
%D3locs gives location of the supposed coals, but not the thicknesses.

%% Build Sands data Set

FullSandSet=honk(:,[2 3 4 5 6 7 8 10 11]);
SandLogDataArray=FullSandSet(indupper:indlower,:);

%% Applying PCA to well data for Sands.
PCDatS = bsxfun(@minus,SandLogDataArray,mean(SandSet));
PCADataArraySand=mtimes(PCDatS,coeffS);

A=size(PCADataArraySand);
Litholog=[PCADataArraySand zeros(A(1,1),1)];

for s=1:A(1,1)
    if ((((PCADataArraySand(s,2)-36.5)-(-19/13)*(PCADataArraySand(s,1)+46.5))^2)/(8^2*(1+(-19/13)^2)))+(((
        LithoLog(s,end)=3;
    end
end

index3=find(LithoLog(:,end)==3);
SandsLocs=DepthInterval(index3);

%% Plotting Data

figure()
plot(DepthInterval,PC3DataC,D3locs,D3pks,'o')
```

```
hold on
plot(SandsLocs,PC3DataC(index3),'green')
xline(13237)
xline(13245.5)
```